

# Standard and Enhanced Cooling of Neutron Stars with Superfluid Cores

K. P. Levenfish and D. G. Yakovlev

*Ioffe Physical Technical Institute ,*

*Russian Academy of Sciences,*

*Politekhnikeskaya 26, St. Petersburg, 194021 Russia*

June 13, 1995

(Published in *Astron. Lett.*, v. 22, No. 1, 56–65, 1996)

## Abstract

Calculations are performed of the cooling of neutron stars with standard and enhanced neutrino energy losses in the presence of neutron and proton superfluidities in the stellar cores. The effects of superfluidity on the heat capacity and the neutrino luminosity produced by the direct and modified Urca processes and by the neutrino bremsstrahlung emission in nucleon-nucleon collisions are taken into account. The constraints are analyzed on the critical temperatures  $T_{cn}$  and  $T_{cp}$  of the transition of neutrons and protons to the superfluid state, which can be obtained from a comparison of observational data on thermal radiation from neutron stars with theoretical cooling curves for the standard and enhanced neutrino energy losses. Possible ranges of  $T_{cn}$  and  $T_{cp}$  for the pulsar Geminga are discussed.

## 1 INTRODUCTION

Neutron stars (NSs) are unique astrophysical objects. The density in the NS central layers is several times higher than the standard nuclear density  $\rho_0 = 2.8 \times 10^{14} \text{ g}\cdot\text{cm}^{-3}$ . Such a dense matter cannot be analyzed in laboratories, but it can be studied by astrophysical methods, in particular, by comparing theoretical calculations of the cooling of NSs with observational data on their thermal emission.

The nuclear composition of the NS central layers is not known with certainty (Shapiro and Teukolsky 1983). We will restrict our consideration to the simplest model in which matter is composed of neutrons ( $n$ ), protons ( $p$ ), and electrons ( $e$ ). The cooling rate of a not-too-old star (with an age  $t < 10^5 \text{ yr}$ ) is determined by the neutrino luminosity of its inner layers. One can

distinguish two types of NSs, with regard to the efficiency of the neutrino energy losses. Stars with a relatively low (*standard*) energy loss rate (see, e.g., Friman and Maxwell 1979; Yakovlev and Levenfish 1995) caused by the modified Urca processes

$$n + N \rightarrow p + N + e + \bar{\nu}_e, \quad p + e + N \rightarrow n + N + \nu_e, \quad (1)$$

and by the bremsstrahlung radiation of neutrino pairs in nucleon-nucleon ( $N$ ) collisions

$$N + N \rightarrow N + N + \nu + \bar{\nu}. \quad (2)$$

constitute the first type of NS.

A buffer nucleon  $N$  in reaction (1) is needed to satisfy momentum conservation in dense matter with relatively low number densities of  $e$  and  $p$ . To avoid misunderstandings, note that we are dealing here with highly degenerate neutrons and protons. The neutron branch of the reaction ( $N = n$ ) is well known; the proton branch ( $N = p$ ) has a comparable intensity, which has been pointed out only recently (Yakovlev and Levenfish 1995). Rather massive NSs whose neutrino luminosity is enhanced by the direct Urca process (Lattimer *et al.* 1991)

$$n \rightarrow p + e + \bar{\nu}_e, \quad p + e \rightarrow n + \nu_e. \quad (3)$$

belong to the second type.

At a not too high density  $\rho \lesssim \rho_0$ , this process is forbidden by momentum conservation.

Observational data on thermal emission from at least three pulsars – PSR 0656 + 14 (Finley *et al.* 1992; Anderson *et al.*, 1993), PSR 0833 – 45 (Ögelman and Zimmermann 1989), and Geminga (Halpern and Holt 1992; Halpern and Ruderman 1993; Meyer *et al.* 1994) – indicate that their cooling is faster than the *standard* cooling but slower than that enhanced by the process (3). In addition, the cooling can be controlled by possible superfluidity of neutrons and/or protons in the stellar core. Superfluidity with a moderate critical temperature  $T_c$  ( $0 < (T_c - T) \lesssim T_c$ , where  $T$  is the temperature of the matter) suppresses the neutrino energy losses but increases the heat capacity through the release of latent heat in a phase transition. Strong superfluidity ( $T_c \gg T$ ) exponentially suppresses both the neutrino losses and the heat capacity of the NS. It is the interplay of these factors that may speed up the standard cooling or slow down the enhanced cooling.

The main parameters of superfluidity that affect the cooling are the critical temperatures  $T_{cn}$  and  $T_{cp}$  of the transition of neutrons and protons, respectively, to a superfluid state. A rigorous calculation of  $T_{cn}$  and  $T_{cp}$  in the core of a NS requires a consistent many-particle quantum theory that adequately describes strong particle interactions. Such a theory has not yet been constructed, but a large number of theoretical models of superdense matter have been proposed. The temperatures  $T_{cn}$  and  $T_{cp}$  calculated in various models (see Wambach *et al.* 1991 and Page 1994 and references therein) vary noticeably with density in the range  $10^7$ – $10^{10}$  K. By comparing observations of thermal emission from isolated NSs with calculations of their cooling at various

temperatures  $T_{cn}$  and  $T_{cp}$ , one can place independent constraints on the parameters of neutron and proton superfluidity in the NS core.

A number of studies are devoted to the models of the standard cooling of a NS with a superfluid core (see, e.g., Nomoto and Tsuruta 1987 and references therein). Page and Applegate (1992) were the first to calculate the cooling enhanced by the direct Urca process in neutron stars with a superfluid core. In these studies, the superfluidity of one nucleon species was considered, and rather approximate fitting formulas describing the effect of superfluidity on the heat capacity and neutrino luminosity were used. A consistent analysis of the effect of  $n$  and  $p$  superfluidity on the heat capacity and neutrino energy losses in the reaction (3) was carried out by Levenfish and Yakovlev (1993). Gnedin and Yakovlev (1993) used these results and, following Page and Applegate (1992), simulated numerically the enhanced cooling of a NS in the presence of neutron or proton superfluidity. The enhanced cooling with both  $n$  and  $p$  superfluidities at once was first considered by Van Riper and Lattimer (1993), who based their analysis on very approximate factors of suppression of the neutrino luminosity by superfluidity. A consistent calculation of the above factors was performed by Levenfish and Yakovlev (1994a,b). Gnedin *et al.* (1994) used these results to model the enhanced cooling of the pulsar PSR 0656 + 14 in the presence of a combined nucleon superfluidity in its core. Comparison of these calculations with observational data on the pulsar's thermal emission allowed the authors to obtain constraints on the critical temperatures  $T_{cn}$  and  $T_{cp}$  in the pulsar's core (assuming that the neutrino energy losses are enhanced by the direct Urca process).

In this paper, we continue to study the cooling of neutron stars with a simultaneous superfluidity of nucleons. Apart from the enhanced cooling, we also consider the standard cooling. The suppression factors for neutrino energy losses required for this consideration have recently been obtained by Yakovlev and Levenfish (1995).

Our models are applied to the pulsar 2CG 195 + 04 (Geminga). The effects of neutron and proton superfluidities on the standard or enhanced cooling of Geminga were first investigated by Page (1994), who used approximate suppression factors for the heat capacity and neutrino energy losses. He showed that observations could be explained for any type of cooling by assuming that the stellar core was superfluid. We develop more detailed models of the NS cooling by including new data on the neutrino energy losses due to the proton branch of the process (1) (Levenfish and Yakovlev 1993, 1994a,b; Yakovlev and Levenfish 1995).

## 2 MODELS OF COOLING NEUTRON STARS

We considered two models of a NS. In both cases, the equation of state of matter ( $npe$ ) in the stellar core was taken from Prakash *et al.* (1988). The maximum mass of the NS for this equation of state is  $1.7 M_{\odot}$ . In the first model, the mass of the star is  $M = 1.44 M_{\odot}$ , the radius is 11.35 km, and the central density is  $\rho_c = 1.37 \times 10^{15} \text{ g}\cdot\text{cm}^{-3}$ . In the second model,  $M = 1.3 M_{\odot}$ ,  $R = 11.71 \text{ km}$ , and  $\rho_c = 1.12 \times 10^{15} \text{ g}\cdot\text{cm}^{-3}$ . The chosen equation of state allows the direct Urca

process to operate at densities  $\rho > \rho_{cr} = 1.30 \times 10^{15} \text{ g}\cdot\text{cm}^{-3}$ . Thus, the first model corresponds to the enhanced cooling: the powerful direct Urca process is possible in a small central kernel with the radius of 2.32 km and mass of  $0.035 M_{\odot}$ . In the second model, the critical density  $\rho_{cr}$  is not achieved, and the star has the standard neutrino luminosity.

We assumed that nucleons could be superfluid throughout the entire NS core. The proton superfluidity results from Cooper pairing of protons in the  $^1S_0$  state, while the neutron superfluidity is due to the neutron pairing in the  $^3P_2$  state with zero projection of the pair's moment onto the quantization axis (see, e.g., Wambach *et al.* 1991). The critical temperatures  $T_{cn}$  and  $T_{cp}$  can depend on density of matter and are not definitely known (Section 1). For certainty, we assumed  $T_{cn}$  and  $T_{cp}$  to be constant throughout the stellar core.

For our cooling calculations, we used the program (Gnedin and Yakovlev 1993; Gnedin *et al.* 1994) in which the inner layers of the NS were assumed to be isothermal. This approximation is valid for a not-too-young NS ( $t > 10\text{--}10^3 \text{ yr}$ ) whose internal thermal relaxation has already occurred. Following Glen and Sutherland (1980), the isothermal region was specified by the condition  $\rho > \rho_b = 10^{10} \text{ g}\cdot\text{cm}^{-3}$ .

The photon luminosity of the NS depends on the effective temperature  $T_e$  of the stellar surface. The relation between  $T_e$  and the temperature  $T_i$  near the boundary of the isothermal region ( $\rho = \rho_b$ ) is determined by the thermal insulation of the outer envelope ( $\rho < \rho_b$ ). The magnetic field in the envelope causes the heat conduction to be anisotropic, resulting in an anisotropic distribution of  $T_e$  over the NS surface (see, e.g., Yakovlev and Kaminker 1994). Even a relatively weak field  $B > 10^{10} \text{ G}$  magnetizes degenerate electrons and reduces the heat conduction across  $\mathbf{B}$ . This enhances the heat insulation of the NS in the vicinity of the magnetic equator. A stronger field,  $B > 10^{12} \text{ G}$ , is quantizing both for a degenerate electron gas in deep layers of the envelope and for nondegenerate sub-photospheric layers. The effects of quantization of electron orbits generally increase the longitudinal thermal conductivity of degenerate electrons, reduce the pressure of degenerate electrons (in the limit of strong quantization), and enhance the radiative thermal conductivity of nondegenerate layers. As a result, the quantizing field weakens the heat insulation near the magnetic poles. The NS cooling has been commonly calculated under the assumption that the magnetic field is radial in every point of the surface (see, e.g., Van Riper 1991 and references therein). In this case, only the reduction of the thermal insulation by the quantizing magnetic field was taken into account. Recently, Shibano and Yakovlev (1996) have considered the cooling of a NS with a dipole field by taking into account both the reduction of the thermal insulation near the magnetic poles and the enhancement of the insulation near the equator. Both effects almost compensate each other for a field strength at the magnetic pole equal to  $B \approx 3 \times 10^{12} \text{ G}$ , and the cooling proceeds in the same way as for  $B = 0$ , although the magnetic field gives rise to a strong anisotropy in  $T_e$ . Our calculations are applied to the Geminga pulsar (Section 1) whose magnetic field is close to the above value (see, e.g., Bertsch *et al.* 1992). Therefore, we neglect the effect of the magnetic field and use the relation between  $T_e$  and  $T_i$  derived by Van Riper (1991) for  $B = 0$ . In this approximation, by  $T_e$  we mean the

average effective surface temperature which determines the total photon luminosity of the star  $L = 4\pi\mathcal{R}^2\sigma T_e^4$  (without allowing for the gravitational redshift). Note that in the calculations of Gnedin *et al.* (1994), like in other calculations in which the magnetic field has been considered to be radial, the influence of the field on the cooling is highly overestimated.

The neutrino luminosity of the NS with  $M = 1.44 M_\odot$  is mainly determined by the direct Urca process (3). The rate of the corresponding neutrino energy losses in normal (nonsuperfluid) matter was calculated by Lattimer *et al.* (1991). Levenfish and Yakovlev (1993) calculated the factors  $R$  of suppression of the reaction (3) by the neutron superfluidity for normal protons ( $R = R_n^{(d)}$ ) and by the proton superfluidity for normal neutrons ( $R = R_p^{(d)}$ ). They also calculated (Levenfish and Yakovlev, 1994b) the suppression of the reaction (3) by both superfluidities ( $R = R_{np}^{(d)}$ ). It turned out that the reaction is mainly suppressed by the strongest superfluidity,  $R_{np}^{(d)} \sim \min[R_n^{(d)}, R_p^{(d)}]$ . Note that Van Riper and Lattimer (1993) used the approximate suppression factors  $R_{np}^{(d)} \sim R_n^{(d)} \cdot R_p^{(d)}$ , which are especially inaccurate if  $R_n^{(d)} \sim R_p^{(d)} \ll 1$ . In addition to the powerful direct Urca process, we also took into account the standard neutrino reactions (1) and (2).

The neutrino luminosity of the  $M = 1.3 M_\odot$  star is determined by both the modified Urca processes (1) and the neutrino emission in nucleon collisions (2) in the entire stellar core. Friman and Maxwell (1979) considered the neutron branch of the modified Urca process (the process (1) for  $N = n$ ) and the bremsstrahlung emission of nucleons (2) in nonsuperfluid matter. Yakovlev and Levenfish (1995) studied the proton branch of the modified Urca process ( $N = p$ ) in non-superfluid matter and showed that this branch was almost as efficient as the neutron branch. Note that the proton branch was commonly considered to be weak and excluded from calculations of the NS cooling. Yakovlev and Levenfish (1995) also calculated the suppression factors of the proton ( $R = R^{(mp)}$ ) and neutron ( $R = R^{(mn)}$ ) branches of the reaction (1) by the neutron superfluidity ( $R_n^{(mn)}$  and  $R_n^{(mp)}$ ) for normal protons and by the proton superfluidity ( $R_p^{(mn)}$  and  $R_p^{(mp)}$ ) for normal neutrons. The suppression factors for the reactions with the same number of superfluid particles turned out to be rather close if they were compared as functions of the corresponding dimensionless energy gap  $v = \Delta_N/T$ . Here,  $\Delta_p$  is the energy gap for the proton (singlet) superfluidity, and  $\Delta_n$  is the minimum energy gap at the Fermi surface of neutrons for the anisotropic (triplet) neutron superfluidity. Thus, for example, the factors  $R_p^{(d)}(v_p)$  and  $R_p^{(mn)}(v_p, v_n)$  are close to each other and to the factors  $R_n^{(d)}(v_n)$  and  $R_n^{(mp)}(v_n)$ . Taking this fact into account, we propose approximate factors of suppression of the neutron ( $R = R_{np}^{(mn)}$ ) and proton ( $R = R_{np}^{(mp)}$ ) branches of the modified Urca process by a combined nucleon superfluidity. One can expect these factors as functions of the corresponding  $v$  (corrected for the number of superfluid particles involved) to be not too different from the factor  $R_{np}^{(d)}$  for the direct Urca process. Therefore, we use the approximate expressions  $R_{np}^{(mp)}(v_p, v_n) \approx R_{np}^{(d)}(2v_p, v_n) R_n^{(mp)}(v_n) / R_n^{(d)}(v_n)$  and  $R_{np}^{(mn)}(v_p, v_n) \approx R_{np}^{(d)}(v_p, 2v_n) R_p^{(mn)}(v_p) / R_p^{(d)}(v_p)$ . If the protons are normal ( $v_p = 0$ ), the expression for  $R_{np}^{(mp)}(v_p, v_n)$  becomes exact, while for normal neutrons ( $v_n = 0$ ) the factor  $R_{np}^{(mn)}(v_p, v_n)$  becomes exact.

The neutrino energy loss rates in the nucleon-scattering processes (2) in nonsuperfluid matter

are taken from Friman and Maxwell (1979). The loss rate in the  $pp$ -scattering is calculated from equation (52) of this paper for the  $nn$ -scattering with the neutron parameters replaced by the proton parameters (see Yakovlev and Levenfish 1995, for details). The factors of suppression of the  $pp$ - ( $R = R_p^{(pp)}$ ) and  $np$ -scattering ( $R = R_p^{(np)}$ ) by the proton superfluidity were calculated by Yakovlev and Levenfish (1995). The similarity relations mentioned above allow us to propose the approximate suppression factors  $R_n^{(nn)}$  for the  $nn$ -scattering by the neutron superfluidity and the suppression factors  $R_{np}^{(np)}$  for the  $np$ -scattering by the combined nucleon superfluidity:  $R_n^{(nn)} \approx R_p^{(pp)}(v_n)$  and  $R_{np}^{(np)} \approx R_{np}^{(d)}(v_p, v_n) R_p^{(np)}(v_p) / R_p^{(d)}(v_p)$ .

Apart from the neutrino luminosity of the NS core, we take into account the neutrino luminosity of the crust resulting from the bremsstrahlung neutrino emission of electrons scattered by atomic nuclei. In this case, the approximate formula proposed by Maxwell (1979) is used.

The heat capacity of the NS is assumed to be the sum of the  $n$ ,  $p$ , and  $e$  heat capacities in the stellar core; we neglect the heat capacity of the crust because the crust mass is low in the chosen NS models. The effects of superfluidity on the  $n$  and  $p$  heat capacities were investigated by Levenfish and Yakovlev (1993). When the superfluidity appears, the heat capacity experiences a jump due to the appearance of the latent heat. The proton (singlet superfluidity) and the neutron (triplet superfluidity) jump abruptly by factors of 2.43 and 2.19, respectively. At  $T \ll T_c$ , the nucleon heat capacity is exponentially suppressed. In our calculations of the neutrino luminosity and heat capacity, we assume the effective masses of neutrons and protons in the NS core to be 0.7 of the masses of bare particles.

### 3 RESULTS

We calculated about 1800 cooling curves for two NS models (Section 2): with the masses  $M = 1.44 M_\odot$  (enhanced cooling) and  $M = 1.3 M_\odot$  (standard cooling). Each curve gives the temporal dependence of the effective surface temperature  $T_s = T_e \sqrt{1 - \mathcal{R}_g / \mathcal{R}}$  of the NS as detected by a distant observer,  $\mathcal{R}_g$  being the gravitational radius of the NS. The curves were calculated in a wide range of critical temperatures of neutrons ( $T_{cn}$ ) and protons ( $T_{cp}$ ) in the NS core (from  $10^7$  to  $10^{10}$  K).

Typical cooling curves are plotted in Fig. 1. Curve 2 corresponds to the standard neutrino losses ( $M = 1.3 M_\odot$ ) in a NS with the normal (nonsuperfluid) core. The change in the shape of the curve at  $t = t_\nu \approx 2.5 \times 10^5$  yr reflects the change of the cooling regime. For  $t \lesssim t_\nu$ , the NS is at the stage of *neutrino* cooling: the neutrino luminosity of the inner stellar layers is considerably higher than the photon luminosity of its surface. For  $t \gtrsim t_\nu$ , the neutrino luminosity falls well below the photon one, and the *photon* stage sets in. Owing to the low neutrino luminosity, the cooling proceeds rather slowly. Curve 1 corresponds to the enhanced neutrino losses ( $M = 1.44 M_\odot$ ) in the NS with a normal core. In this case, the NS cools much faster, with the neutrino-cooling stage being slightly delayed. The duration  $t_\nu$  of the neutrino stage is mainly determined by the stellar heat capacity and by the dependence of the neutrino luminosity on the NS core temperature. For

normal nucleons,  $t_\nu \sim (2-4) \times 10^5$  yr. A strong proton superfluidity with normal neutrons reduces the heat capacity and time  $t_\nu$  by about (20–30)%. For a strong neutron superfluidity and normal protons, the heat capacity and  $t_\nu$  decrease by a factor of 2 to 3. In the case of strong  $n$  and  $p$  superfluidities, the heat capacity drops approximately by a factor of 20, and  $t_\nu \sim 10^4$  yr.

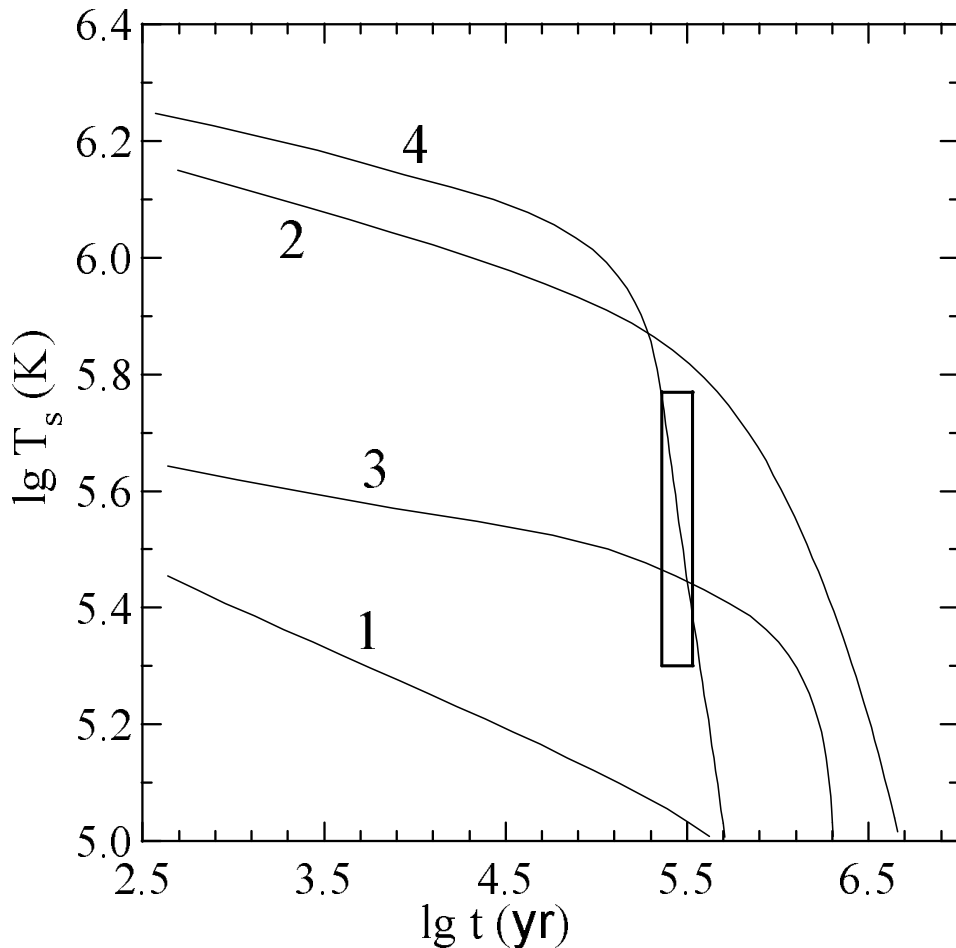


Figure 1: Cooling curves for a neutron star with enhanced (curves 1 and 3) and standard (curves 2 and 4) neutrino luminosities. Curves 1 and 2 correspond to the absence of superfluidity; curve 4 to  $T_{cn} = 10^{9.5}$  K,  $T_{cp} = 10^{8.5}$  K; and curve 3 to  $T_{cn} = 10^{7.3}$  K,  $T_{cp} = 10^{8.5}$  K. The rectangle encloses the region of the selected effective surface temperatures  $T_e$  and Geminga's ages  $t$ .

The results of our calculations are of general character. We will analyze them using the Geminga pulsar as an example. Recent observations of Geminga from the ROSAT X-ray Orbital Observatory provide a wealth of information on the X-ray emission of this pulsar (Halpern and Holt 1992; Halpern and Ruderman 1993; Meyer *et al.* 1994). The emission consists of soft and hard components. The soft component is interpreted as the thermal emission from the Geminga surface, while the hard component is commonly attributed to the emission of small hot spots on

the stellar surface. Theoretical interpretation of the observational data is ambiguous. Thus, for example, Halpern and Ruderman (1993) described the soft and hard components by blackbody spectra with different temperatures and estimated the effective surface temperature to be  $T_e = (5.2 \pm 1.0) \times 10^5$  K. The same authors fitted the soft and hard components with a blackbody spectrum and a power-law spectrum, respectively. In this model,  $T_e = (4.5 \pm 1.4) \times 10^5$  K. Meyer *et al.* (1994) interpreted the emission of the hard component using a set of NS hydrogen-atmosphere models with a magnetic field. The best-fit models are consistent with a lower temperature,  $T_e = (2-3) \times 10^5$  K. Recently, Page *et al.* (1995) have interpreted the spectroscopic observations of Geminga using the model of a cool hydrogen nonmagnetic atmosphere ( $T_e \approx 2.2 \times 10^5$  K) without a magnetic field in the presence of two small hot spots ( $4 \times 10^5$  K) with a radial magnetic field of opposite polarity. It should be stressed that the modeling of NS atmospheres is far from being complete. It is necessary to solve a complicated problem of radiative transfer in a magnetized, sufficiently cool and dense (nonideal) plasma of the NS atmosphere with a complex chemical composition (hydrogen, helium, and heavy elements). It is quite possible that new models and observational data will yield slightly different values of  $T_e$ . We will not favor any of the available interpretations, but consider the temperature  $T_e$  as an unknown quantity. We will take  $T_e = (2-6) \times 10^5$  K as the most plausible temperature  $T_s$  (with allowance for the gravitational redshift). For the  $M = 1.3 M_\odot$  and  $M = 1.44 M_\odot$  models, the  $T_s/T_e$  ratios are equal to 0.820 and 0.791, respectively.

The age of Geminga is estimated (Bertsch *et al.* 1992; Page 1994) from the observed rotation period  $P \approx 0.237$  s and its time derivative  $\dot{P} = 1.10 \times 10^{-14}$  s/s using the well-known formula  $t = (P/\dot{P})/(n-1)$ , where  $n$  is the braking index. For the magnetic-dipole losses ( $n = 3$ ),  $t = t_1 = 3.4 \times 10^5$  yr. For  $n = 4$ , we have  $t = t_2 = 2.3 \times 10^5$  yr, which may be considered as the lower limit of the Geminga's age (Page 1994).

We will assume the ranges of surface temperatures  $T_s = (2-6) \times 10^5$  K and ages  $t_2 \leq t \leq t_1$  (Fig. 1) to form an "error box" which the real cooling curves of the Geminga pulsar must intersect. One can see that in the absence of superfluidity, the cooling proceeds more slowly than required for the standard neutrino luminosity and more rapidly than required for the enhanced luminosity. A detailed analysis made by Page (1994) has shown that both the standard and enhanced neutrino luminosities fit the observations if the effect of superfluidity is taken into account. This assertion is illustrated by curves 3 and 4 in Fig. 1. Curve 3 corresponds to the standard neutrino energy losses ( $M = 1.3 M_\odot$ ) at  $T_{cn} = 10^{9.5}$  K and  $T_{cp} = 10^{8.5}$  K. Such a superfluidity decreases strongly the heat capacity of the star and accelerates the cooling at the photon stage (when the superfluid suppression of the neutrino luminosity is insignificant). Curve 4 corresponds to the enhanced neutrino luminosity ( $M = 1.44 M_\odot$ ) at  $T_{cn} = 10^{7.3}$  K and  $T_{cp} = 10^{8.5}$  K. The superfluidity chosen suppresses the neutrino luminosity more strongly than the heat capacity, and delays the cooling at the neutrino stage and at the transition stage from the neutrino to photon cooling.

With the inclusion of new data on neutrino energy losses and the NS heat capacity (Sections 1 and 2), our calculations extend the study of Page (1994) to a wider range of  $T_{cn}$  and  $T_{cp}$ . In view



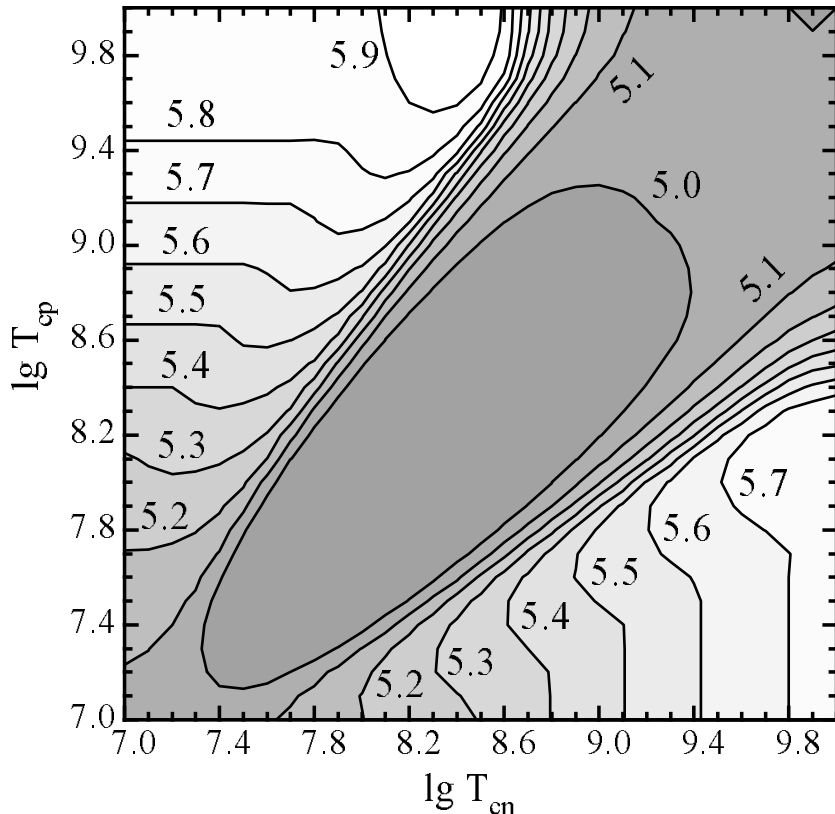


Figure 2:  $T_{cn}$  and  $T_{cp}$  lines corresponding to certain surface temperatures  $T_s$  of a neutron star with the enhanced neutrino luminosity ( $M = 1.44 M_\odot$ ) and age of  $3.4 \times 10^5$  yr. The numbers near the curves are the values of  $\log T_s$ .

of the great variety of the results, their representation by cooling curves is inconvenient. It is more convenient (Gnedin *et al.* 1994) to display the critical superfluidity temperatures  $T_{cn}$  and  $T_{cp}$  which lead to definite effective surface temperatures  $T_s$  of a NS of given age  $t$  (Figs. 2–5). Figures 2 and 4 correspond to the age  $t_1$ , while Figs. 3 and 5 correspond to the age  $t_2$ .

Figures 2 and 3 correspond to enhanced neutrino energy losses. Since the figures are similar, we will describe Fig. 2 ( $t = t_1$ ) as an example. The lower left corner of this figure corresponds to the case where the critical temperatures  $T_{cn}$  and  $T_{cp}$  are below or of the same order of magnitude as the internal temperature of a NS of age  $t_1$ . The nucleon superfluidity either has not yet appeared in or has had no time to strongly affect the cooling. As a result, the NS surface temperature drops to  $\sim 10^5$  K (Fig. 1) through intense neutrino energy losses in the direct Urca process, with the star being still at the neutrino cooling stage ( $t_\nu \gtrsim t_1$ ).

In all the remaining parts of Fig. 2, the effect of superfluidity on the cooling turns out to be crucial. Calculations and a simplified analytic analysis of the cooling equations show that  $t_\nu \sim t_1$  throughout the figure (with the exception of the upper right corner of Fig. 2). In that

case, the cooling is governed by both the neutrino luminosity and the heat capacity of the NS. The neutron superfluidity affects the direct Urca process and the proton heat capacity in about the same manner as the proton superfluidity affects the direct Urca process and the proton heat capacity (Levenfish and Yakovlev 1994a,b). In addition, the heat capacities of normal neutrons and protons are comparable but considerably larger than the electron heat capacity. As a result, the curves in Fig. 2 are almost symmetric with respect to the replacement of the coordinate axes,  $\log T_{cn} \leftrightarrow \log T_{cp}$ , and it is sufficient, for instance, to describe the lower right half of Fig. 2.

If a low temperature of  $T_{cp} \sim 10^7$  K is fixed and  $T_{cn}$  increases from  $\sim 10^8$  to  $\sim 10^{10}$  K, the proton superfluidity does not occur by the time  $t_1$ , and the cooling is governed by the neutron superfluidity alone. Therefore, the  $T_s = \text{const}$  lines in the lower right corner of Fig. 2 are vertical. As  $T_{cn}$  increases, the neutrino luminosity drops by several orders of magnitude. The heat capacity also changes but much weaker, because the strong  $n$  superfluidity reduces the NS heat capacity only by a factor of approximately 3. As a result, variations in the neutrino luminosity are more pronounced than variations in the heat capacity. The cooling of the star slows down, while  $T_s$  rises. If, on the other hand, we fix  $T_{cn} \gtrsim 10^8$  K and increase  $T_{cp}$ , then the  $p$  superfluidity will arise in a star of age  $t_1$  at some value of  $T_{cp}$  (and the  $T_s = \text{const}$  line will no longer be straight). As  $T_{cp}$  increases further, the superfluidity suppresses the neutrino luminosity and influences the heat capacity. However, the additional suppression of the direct Urca process by a moderate proton superfluidity in the presence of a strong neutron superfluidity is weaker than the change in the proton heat capacity (Levenfish and Yakovlev 1994a,b). Then the cooling is mainly controlled by the proton heat capacity. When the superfluidity arises, the heat capacity increases in a jump-like manner (the latent heat is liberated), giving rise to an increase in  $T_s$ : the  $T_s = \text{const}$  lines are shifted leftward. However, the increase in the heat capacity is superseded by its sharp suppression with rising  $T_{cp}$ . The NS becomes cooler, and the isolines are shifted rightward.

Finally, the critical temperatures  $T_{cn}$  and  $T_{cp}$  in the upper right corner of Fig. 2 are so large that the neutron and proton superfluidities suppress the direct Urca process and the nucleon heat capacity almost completely. For a very low (electron) heat capacity, the neutrino-cooling stage is short ( $t_\nu \sim 10^4$  yr, see above). As a result, the NS had long cooled down by the time  $t_1$  through the photon emission, and its temperature is very low,  $T_s \sim 10^5$  K.

Figures 2 and 3, corresponding to the enhanced cooling of Geminga, are similar to Figs. 2, 4, and 6 from Gnedin *et al.* (1994) composed for the younger pulsar PSR 0656 + 14 ( $t \approx 10^5$  yr). A comparison of these figures shows that higher critical temperatures of one of the nucleon components under the condition  $T_{cp} \ll T_{cn}$  or  $T_{cn} \ll T_{cp}$  are required for maintaining the high effective temperature  $T_s$  over a longer period of time.

$T_s$  isolines for the NS model with  $M = 1.3 M_\odot$  are plotted in Figs. 4 and 5. Figures 4 and 5 correspond to the ages  $t_1$  and  $t_2$ , respectively. It can be seen that the behavior of the isolines for the standard neutrino energy losses differs qualitatively from that for the enhanced neutrino energy losses (Figs. 2 and 3). The principal difference lies in the fact that the relatively weak standard neutrino luminosity of a NS of age  $t_1$  or  $t_2$  turns out to be lower than the photon

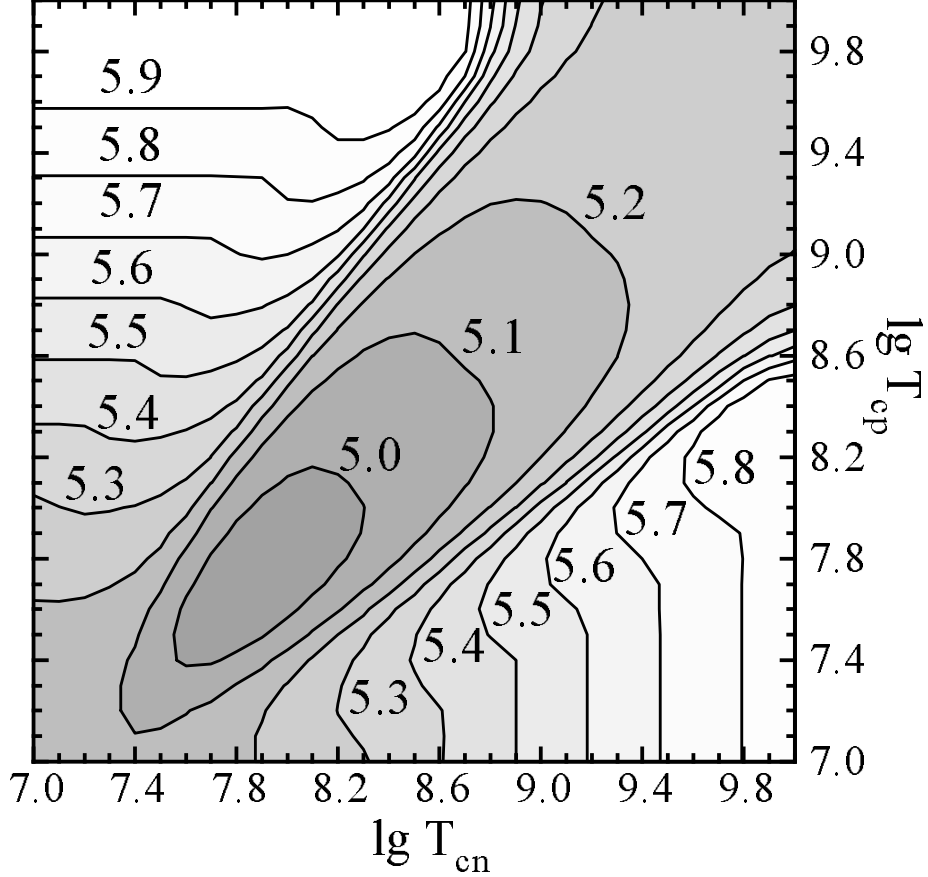


Figure 3: Same as in Fig. 2 but for a star of age  $t = 2.3 \times 10^5$  years.

luminosity ( $t_\nu \lesssim t_2$ ). The NS of the above age is at the photon-cooling stage virtually for all values of  $T_{cn}$  and  $T_{cp}$  shown in Figs. 4 and 5, and the neutrino luminosity of the stellar core plays no significant role. The nucleon superfluidity affects the cooling mainly through the heat capacity. The exception is only some small parts of Figs. 4 and 5.

Figures 4 and 5 are qualitatively similar. We will describe Fig. 4 as an example. At  $T_{cn} < 10^{7.9}$  K and  $T_{cp} < 10^{7.9}$  K (lower left corner of Fig. 4), the nucleon superfluidity in the core of a NS of age  $t_1$  has not yet appeared, and the surface temperature is independent of  $T_{cn}$  and  $T_{cp}$ . At  $T_{cp} \lesssim 10^{7.5}$  K (lower part of Fig. 4), the protons are normal. If, at the same time, we raise  $T_{cn}$ , the neutron superfluidity will arise at  $T_{cn} > 10^{7.9}$  K by the time  $t_1$ . At  $T_{cn} \lesssim 10^8$  K, this superfluidity is moderate. The latent heat is released, and  $T_s$  slightly rises. As  $T_{cn}$  increases further, the  $n$  superfluidity becomes strong by the time  $t_1$ ; it sharply suppresses the neutron heat capacity, and decreases  $T_s$ . As  $T_{cn}$  rises, the  $n$  superfluidity arises increasingly earlier. At  $T_{cn} \sim 10^9$  K, it appears at the early neutrino-cooling stage and is able to strongly suppress the neutrino losses and delay the cooling. Though weakly, this delay manifests itself by the time  $t_1$ : as  $T_{cn}$  becomes higher than  $10^9$  K, the temperature  $T_s$  slightly rises. If, however, we fix  $T_{cn} \sim 10^9$  K and raise  $T_{cp}$ , the  $p$  superfluidity arises at  $T_{cp} \gtrsim 10^{7.6}$  K. The latent heat is released, and  $T_s$  grows. As a result, the  $T_s = \text{const}$  lines in Fig. 4 form loops (e.g.,  $\log T_s = 5.7$ ).

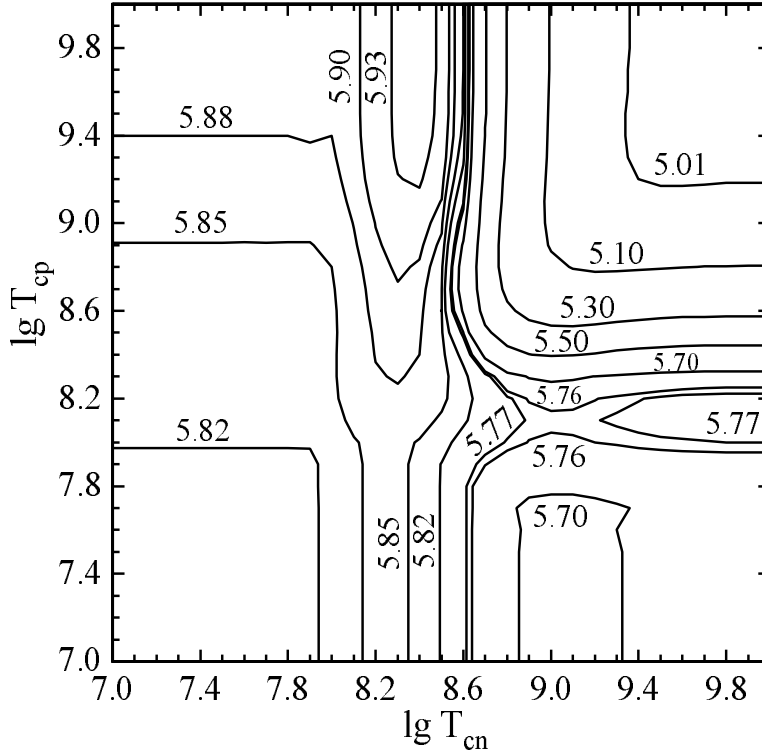


Figure 4: Same as in Fig. 2 but for a star with standard neutrino luminosity.

At  $T_{cn} \lesssim 10^{7.9}$  K (left part of Fig. 4), the neutrons are normal. If  $T_{cp}$  is raised above  $\gtrsim 10^{7.9}$  K, the proton superfluidity appears by the time  $t_1$ . At  $T_{cp} \sim 10^8$  K, the superfluidity arises just before  $t_1$  and is moderate. The heat capacity increases due to the latent-heat release, and  $T_s$  slightly rises. As  $T_{cp}$  grows further, the  $p$  superfluidity arises at increasingly earlier stages and becomes strong by the time  $t_1$ . It suppresses the proton heat capacity, which amounts to  $\lesssim 30\%$  of the total heat capacity of the NS for normal neutrons. On the other hand, this superfluidity exponentially suppresses the neutrino luminosity at the preceding neutrino-cooling stage. The slowdown of the cooling due to the suppression of the neutrino luminosity is more pronounced than the acceleration caused by an insignificant suppression of the heat capacity, and  $T_s$  rises with increasing  $T_{cp}$ .

At  $T_{cp} \gtrsim 10^9$  K (upper part of Fig. 4), the  $p$  heat capacity is suppressed completely. If  $T_{cn}$  is raised, the  $n$  superfluidity appears by the time  $t_1$ , which first enhances and then suppresses the  $n$  heat capacity (see above). This causes  $T_s$  to initially rise and then decrease with a peak at  $T_{cn} \approx 10^{8.3}$  K. If  $T_{cn} \approx 10^{8.3}$  K is fixed and  $T_{cp}$  decreases,  $T_s$  slightly drops. This drop of  $T_s$  is caused by the enhancement of the stellar neutrino luminosity at the preceding neutrino-cooling stage. As a result, the  $\log T_s = 5.9$  curve forms, for example, a loop in the upper part of Fig. 4. The  $\log T_s = 5.77$  loop in the right part of Fig. 4 is explained in a similar way (with replacement  $n \leftrightarrow p$ ).

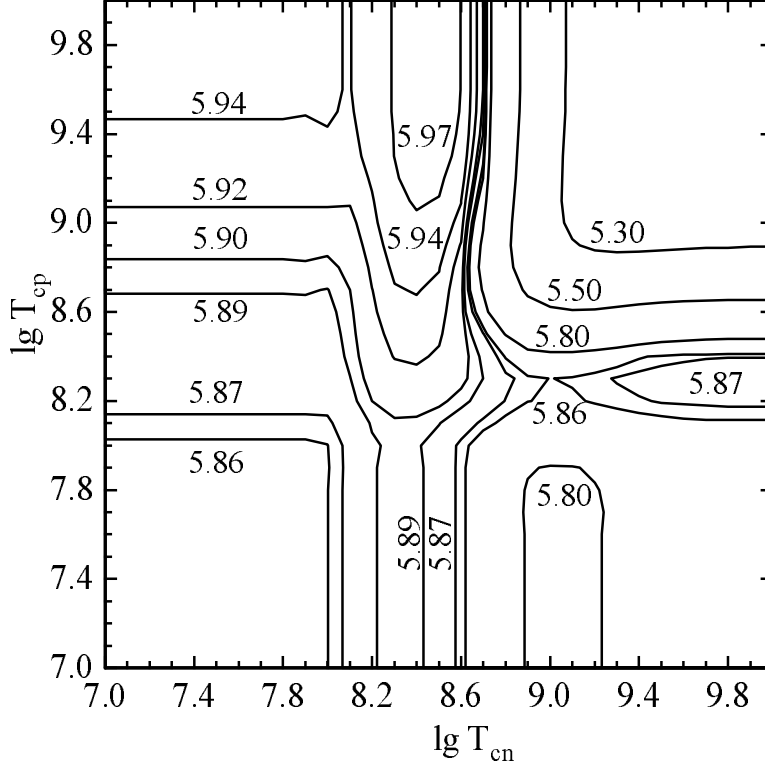


Figure 5: Same as in Fig. 3 but for the star with enhanced neutrino luminosity.

Finally, at  $T_{cn} \gtrsim 10^{8.6}$  K and  $T_{cp} \gtrsim 10^{8.3}$  K (upper right part of Fig. 4), the  $n$  and  $p$  superfluidities become strong by the time  $t_1$  and heavily suppress the nucleon heat capacity. The neutrino-cooling stage is considerably shorter ( $t_\nu \ll t_1$ , see above), and the  $T_s = \text{const}$  curves are entirely determined by a decrease in the heat capacity caused by superfluidity. The higher  $T_c$ , the lower the heat capacity, and the cooler the star. At  $T_{cn} \gtrsim 10^{9.2}$  K, the  $n$  superfluidity suppresses the neutron heat capacity almost completely, and the cooling is governed only by a change in  $T_{cp}$  (proton heat capacity) at  $T_{cp} \lesssim 10^9$  K. If, however,  $T_{cp} \gtrsim 10^9$  K, the  $p$  superfluidity suppresses the proton heat capacity almost completely, and the cooling is governed by a change in  $T_{cn}$  (neutron heat capacity) at  $T_{cn} \lesssim 10^{9.2}$  K. If the combined superfluidity of neutrons and protons is very strong ( $T_{cn} > 10^{9.2}$  K,  $T_{cp} > 10^{9.1}$  K, see the uppermost right corner of Fig. 4), the nucleon heat capacity of the NS core is fully suppressed, and the cooling no longer depends on  $T_{cn}$  and  $T_{cp}$ . In this regime, the cooling is governed by the electron heat capacity, which is independent of the nucleon superfluidity.

It should be emphasized that the  $T_s = \text{const}$  curves at  $T_{cn} \gtrsim 10^{8.5}$  K and  $T_{cp} \gtrsim 10^{8.3}$  K (upper right part of Fig. 4) are determined by an abrupt suppression of the heat capacity by strong superfluidity and are only slightly sensitive to the specific parameters of the NS. In the remaining region of  $T_{cn}$  and  $T_{cp}$ , variations in  $T_s$  are small, but the  $T_s = \text{const}$  curves (for instance, loops)

may formally strongly deform with changing NS parameters (cf., the  $\log T_s = 5.7$  and  $\log T_s = 5.8$  isolines in Figs. 4 and 5). This deformation is not accompanied by large variations in  $T_s$  and does not affect the main conclusions concerning the effect of superfluidity on the cooling.

Note that Page (1994) considered a wider age range for Geminga,  $t_2 \leq t \leq t_3$ , where  $t_3 = 6.8 \times 10^5$  yr corresponds to the braking index  $n = 2$  (see above). We give no results for  $t = t_3$ . In the case of the enhanced neutrino losses, the corresponding figures are similar to Figs. 2 and 3. In the case of the standard energy losses, at  $t = t_3$ , Geminga is at the advanced photon-cooling stage, when the surface temperature is sufficiently low ( $T_s \approx 5.7 \times 10^5$  K) even for normal nucleons (Fig. 1).

## 4 CONCLUSIONS

Our calculations support the conclusion of Page (1994): observational data on the thermal emission of Geminga can be explained by both the standard or enhanced neutrino energy losses if neutrons and protons in the Geminga's core are assumed to be superfluid. Figures 2 and 3 give the critical temperatures of the neutron and proton superfluidities,  $T_{cn}$  and  $T_{cp}$ , which lead to specified effective surface temperatures  $T_s$  of Geminga if its age is  $t_1 = 3.4 \times 10^5$  yr or  $t_2 = 2.3 \times 10^5$  yr (Section 3) and the neutrino luminosity is enhanced by the direct Urca process (3). Figures 4 and 5 are similar but correspond to the assumption that the neutrino luminosity is standard and results from the reactions (1) and (2). Observational data on the X-ray emission of Geminga (Section 3) indicate that its effective surface temperature  $T_s$  ranges from  $2 \times 10^5$  K to  $6 \times 10^5$  K.

Both assumptions about the neutrino energy losses (standard and enhanced) can be reconciled with observational data. In both cases, the required values of  $T_{cp}$  and  $T_{cn}$  are in qualitative agreement with various model calculations of the critical temperatures of nucleon superfluidity in NS cores (see Page and Applegate 1992, for references). However, the properties of superfluidity in the Geminga's core for the standard and enhanced neutrino luminosities must greatly differ. In the case of the enhanced neutrino luminosity, the superfluidity is needed to slow down the NS cooling at the neutrino-cooling stage (or at the transition stage from the neutrino to photon luminosity) through a partial suppression of the neutrino energy losses in the direct Urca process. For example, the values of  $T_{cn}$  and  $T_{cp}$  that give the Geminga's surface temperature  $T_s = 10^{5.3-10^{5.5}}$  K lie (see Figs. 2 and 3) in two relatively wide decoupled regions in the  $(T_{cn}-T_{cp})$  plane. For the standard neutrino processes, the superfluidity must slow down the cooling at the photon-cooling stage through the suppression of the stellar heat capacity. The region of the necessary values of  $T_{cn}$  and  $T_{cp}$  (Figs. 4 and 5) turns out to be much narrower and coupled. For the same  $T_s$ , we obtain  $\log T_{cn} \gtrsim 8.7$  and  $\log T_{cp} \gtrsim 8.5$ . In this case, the constraints on possible values of critical temperatures are much more stringent. On the whole, the model of the standard neutrino losses requires higher  $T_{cn}$  and  $T_{cp}$  than the model of the enhanced losses.

The results of our calculations are tentative. More detailed models for the cooling of NSs with superfluid cores are needed. First, it would be desirable to allow for the nonuniform distribution

of the critical temperatures  $T_{cn}$  and  $T_{cp}$  (for their density dependence) throughout the stellar core. For this to be done, joint theoretical calculations of  $T_{cn}$  and  $T_{cp}$  are necessary for various models of superdense matter (which are now not available). These data could be used to directly determine the best-fit models without assuming that  $T_{cn}$  and  $T_{cp}$  are free parameters. It would be desirable to consider the cases where other particles, above all, muons and hyperons, are present in the NS cores along with neutrons, protons and electrons. Note that the neutrino-loss rates in various types of reaction are also sensitive to superdense-matter models and have not yet been determined with confidence. At the late cooling stage, additional heating sources may also be important, for example, those related to dissipation of the rotational energy in the core of a star during its slowdown (see, e.g., Cheng *et al.* 1992, Umeda *et al.* 1994, and references therein). One may hope that new observational data on the thermal emission of NSs together with new theoretical calculations will make it possible to obtain more stringent constraints on the rate of neutrino energy losses and the critical temperatures of nucleon superfluidity in superdense matter.

#### ACKNOWLEDGMENTS

We wish to thank O.Yu. Gnedin for useful discussions and great assistance in our calculations, and to V.S.Imshennik and Yu.A. Shibarov for valuable critical remarks. This work was supported in part by the Russian Basic Research Foundation (project code 93-02-2916), the Soros International Science Foundation (Grant R6A-000), the ESO C&EE Programme (Grant A-01-068) and by INTAS (Grant 94-3834).

#### REFERENCES

- Anderson, S.B., Córdoba, F.A., Pavlov, G.G., *et al.*, *Astrophys. J.*, 1993, v. 414, p. 867.  
 Bertsch, D.L., Brazier, K.T.S., Fichtel, C.E., *et al.*, *Nature*, 1992, v. 357, p. 306.  
 Cheng, K.S., Chau, W.Y., Zhang, J.L., and Chau, H.F., *Astrophys. J.*, 1992, v. 396, p. 135.  
 Finley, J.P., Ögelman, H., and Kiziloglu, Ü., *Astrophys. J.*, 1992, v. 394, p. L21.  
 Friman, B.L. and Maxwell, O.V., *Astrophys. J.*, 1979, v. 232, p. 541.  
 Glen, G. and Sutherland, P., *Astrophys. J.*, 1980, v. 239, p. 671.  
 Gnedin, O.Yu. and Yakovlev, D.G., *Astron. Lett.*, 1993, v. 19, p. 104.  
 Gnedin, O.Yu., Yakovlev, D.G., and Shibarov, Yu.A., *Astron. Lett.*, 1994, v. 20, p. 409.  
 Halpern, J.P. and Ruderman, M., *Astrophys. J.*, 1993, v. 415, p. 286.  
 Halpern, J.P. and Holt, S.S., *Nature*, 1992, v. 357, p. 222.  
 Lattimer, J.M., Pethick, C.J., Prakash, M., and Haensel, P., *Phys. Rev. Lett.*, 1991, v. 66, p. 2701.  
 Levenfish, K.P. and Yakovlev, D.G., Strongly Coupled Plasma Physics, Van Horn, H. and Ichimaru, S., Eds., Rochester: University Rochester, 1993, p. 167.  
 Levenfish, K.P. and Yakovlev, D.G., *Astron. Lett.*, 1994a, v. 20, p. 43.  
 Levenfish, K.P. and Yakovlev, D.G., *Astron. Rep.*, 1994b, v. 38, p. 247.

- Maxwell, O.V., *Astrophys. J.*, 1979, v. 231, p. 201.
- Meyer, R.D., Pavlov, G.G., and Mészáros, P., *Astrophys. J.*, 1994, v. 433, p. 265.
- Nomoto, K. and Tsuruta, S., *Astrophys. J.*, 1987, v. 312, p. 711.
- Ögelman, H. and Zimmermann, H.-U., *Astron. Astrophys.*, 1989, v. 214, p. 179.
- Page, D., *Astrophys. J.*, 1994, v. 428, p. 250.
- Page, D. and Applegate, J.H., *Astrophys. J. Lett.*, 1992, v. 394, p. L17.
- Page, D., Shibano, Yu.A., and Zavlin, V.E., *Astrophys. J. Lett.*, 1995, v. 451, L21.
- Prakash, M., Ainsworth, T.L., and Lattimer, J.M., *Phys. Rev. Lett.*, 1988, v. 61, p. 2518.
- Shapiro, S.L. and Teukolsky, S.A., *Black Holes, White Dwarfs, and Neutron Stars*, New York: Wiley, 1983.
- Shibano, Yu.A. and Yakovlev, D.G., *Astron. Astrophys.*, 1996, v. 309, p. 171.
- Umeda, H., Tsuruta, S., and Nomoto, K., *Astrophys. J.*, 1994, v. 433, p. 256.
- Van Riper, K.A. and Lattimer, J.M., in: *Isolated Pulsars*, Van Riper, K.A. and Epstein, R., Eds., Cambridge: Cambridge Univ., 1993, p. 122.
- Van Riper, K.A., *Astrophys. J., Suppl. Ser.*, 1991, v. 75, p. 449.
- Wambach, J., Ainsworth, T.L., and Pines, D., in: *Neutron Stars: Theory and Observation*, Ventura, J. and Pines, D., Eds., Dordrecht: Kluwer Acad., 1991, p. 37.
- Yakovlev, D.G. and Kaminker, A.D., in: *Equations of State in Astrophysics*, Chabrier, G. and Schatzman, E., Eds., Cambridge: Cambridge Univ., 1994, p. 214.
- Yakovlev, D.G. and Levenfish, K.P., *Astron. Astrophys.*, 1995, v. 297, p. 717.